High-Temperature, High-Pressure Viscosities and Densities of n-Hexadecane, 2,2,4,4,6,8,8-Heptamethylnonane and Squalane Measured Using a Universal Calibration for a Rolling-Ball Viscometer/Densimeter

Aaron J. Rowane[a,b,*], Rajendar R. Mallepally[c], Ashutosh Gupta[d], Manolis Gavaises[a], Mark A. M[c]Hugh[c]

[a] Department of Mechanical Engineering and Aeronautics, City University of London, Northampton Square, ECIV 0HB London (UK)

[b] Afton Chemical Limited, London Rd, Bracknell, RG12 2UW, Berkshire (UK)

[c] Department of Chemical and Life Science Engineering, Virginia Commonwealth University, Richmond, VA 23220 (USA)

[d] Afton Chemical Corporation, 500 Spring Street, Richmond, Virginia, 23219 (USA)

* Corresponding author; e-mail: aaron.rowane@aftonchemical.com

Abstract

The development of reference correlations for viscous fluids is predicated on the availability of accurate viscosity data, especially at high pressure, high temperature (HPHT) conditions. The rolling ball viscometer (RBV) is a facile technique for obtaining such HPHT viscosity data. A new, universal RBV calibration methodology is described and applied over a broad *T*-*p* region and for a wide range of viscosities. The new calibration equation is used to obtain viscosities for n-hexadecane (HXD), 2,2,4,4,6,8,8-heptamethylnonane (HMN), and 2,6,10,15,19,23-hexamethyltetracosane (squalane) from 298 – 530 K and pressures to 250 MPa. The available literature data base for HMN is expanded to 520 K and 175 MPa and for squalane to 525 K and 250 MPa. The combined expanded uncertainties are 0.6% and 2.5% for the densities and viscosities, respectively, each with a coverage factor, $k = 2$. The reliability of the viscosity data is validated by comparison of HXD and squalane viscosities to accepted reference correlations and HMN viscosities to available literature data. The necessity of this new calibration approach is confirmed by the large deviations observed between HXD, HMN, and squalane viscosities determined using the new, universal RBV calibration equation and viscosities determined using a quadratic polynomial calibration equation. HXD, HMN, and squalane densities are predicted with the Perturbed Chain Statistical Associating Fluid Theory using pure component parameters calculated with a previously reported group contribution (GC) method. HXD, HMN, and squalane viscosities are compared to Free Volume Theory (FVT) predictions using FVT parameters calculated from a literature correlation for n-alkanes. Although the FVT predictions for HXD, a normal alkane, result in an average absolute percent deviation (Δ_{AAD}) of 3.8%, predictions for HMN and squalane, two branched alkanes, are four to 13 times larger. The fit of the FVT model for the branched alkanes is dramatically improved if the FVT parameters are allowed to vary with temperature.

Keywords: Squalane, Hexadecane, 2,2,4,4,6,8,8-heptamethylnonane, Rolling-Ball Viscometer Calibration, High Pressure Viscosity, High Pressure Density, Free Volume Theory, PC-SAFT

1. Introduction

Accurate thermophysical fluid properties are crucial for the design and operation of chemical processes used to manufacture specialty chemicals, lubricants, crude oil, polymers, etc. [1, 2]. The need for a fluid property database is especially important when operating at high-pressure, high-temperature (HPHT) conditions, such as those encountered in the recovery of petroleum reserves in ultra-deep reservoirs, in the application of lubricants to reduce energy losses due to friction in the automotive and allied industries, and in the operation of highly efficient diesel engines designed to reduced soot emissions. A well-developed HPHT property data base with an emphasis on viscosity information is also crucial for the development and refinement of reference correlations. HPHT viscosity predictions for oils, lubricants, and fuels are particularly challenging given that these fluids often contain tens to hundreds of components differing in molecular weight and structure. Here we address the experimental challenge to measure HPHT viscosity for normal and branched alkanes, two components typically found in fuels.

The apparatus used to measure HPHT viscosities fall into two general categories. One type of apparatus is classified as an absolute measurement technique that does not require calibration with a fluid of known properties. The vibrating-wire viscometer[3-6] and quartz crystal resonator viscometer[7] are two absolute measurement apparatus that provide very high precision data to within 0.5 to 2.0%, without the need for calibration. However, these techniques typically rely on sensitive electronics directly interfaced with the measurement apparatus and, thus, are limited to modest operating temperatures. The second type of measurement apparatus is a relative technique since this apparatus does require calibration. The most common relative viscosity measurement

techniques are the falling-body viscometer (FBV)[7, 8], rolling-ball viscometer (RBV) [9-12], and rolling-ball viscometer/densimeter (RBVD)[13, 14]. These apparatus can be used without sensitive electronics and, therefore, can be readily operated at temperatures well in excess of 473 K. Note that the viscosity calibration method presented here is identical for both an RBV and an RBVD used in our experimental studies. Therefore, the acronym RBVD is used exclusively in the following sections.

A typical RBVD calibration method is to use available reference viscosity data to determine a calibration parameter over the entire *T-p* region of interest [9, 10, 13, 15] and fit the resultant data to a polynomial function of temperature and pressure. However, it is well documented that relative viscosity measurement techniques require a reference fluid having a viscosity profile similar to that of the fluid to be measured. This consideration can lead to multiple calibration experiments when measuring viscosities for fluids of the same chemical family but with different molecular weights, such as octane and hexadecane. Not only are multiple calibration measurements time consuming, they are problematic as noted by Tomida et al.[16] and Paredes et al.[11] who both stress the lack of available calibration fluids having data over broad *T-p* regions, especially for highly viscous fluids. Assael and coworkers[17] further argue that more data are needed to develop suitable reference correlations for viscous fluids and the new viscosity data should be obtained at extreme HPHT conditions where data are particularly scarce.

Here a general RBVD calibration equation is developed that is valid over a broad *T-p* region and that can be used for normal and branched hydrocarbons such as octane, decane, hexadecane, heptamethylnonane, and squalane. The derived RBVD calibration equation is used for viscosity measurements at temperatures to 530 K and pressures 250 MPa for n-hexadecane (HXD), 2,2,4,4,6,8,8-heptamethylnonane (HMN), and 2,6,10,15,19,23-hexamethyltetracosane

(squalane), which exhibit viscosities from 0.4 to 1200 mPa•s in the *T-p* region studied here. HXD and squalane viscosities are compared to accepted reference correlations[18, 19] and available literature data[4, 6-8, 11, 12, 16, 20-30] and HMN data are compared to available literature data[27, 31-37] to validate the calibration approach. The necessity of the new RBVD calibration equation is demonstrated with a direct comparison of HXD, HMN, and squalane viscosity data obtained in the present study with viscosities obtained using a quadratic polynomial calibration equation. The resultant viscosity data are modeled using the Free Volume Theory (FVT) for which the input densities are predicted from the Perturbed Chain Statistical Associating Fluid Theory (PC-SAFT) equation of state (EoS).

2. Materials and Methods

2.1. Materials

Table 1 lists the source and mass fraction purity of each chemical used, as received, in this study.

Table 1. Chemical samples used in this study listed with the source and mass fraction purity reported by the manufacturer.

Chemical Name	Source	Mass Fraction Purity
n-Octane	Sigma-Aldrich	≥ 0.990
n-Decane	Sigma-Aldrich	≥ 0.990
n-Hexadecane	Sigma-Aldrich	0.990
2,2,4,4,6,8,8-Heptamethylnonane	Acros Organics	0.980
Squalane	Acros Organics	0.990

2.2 Rolling–Ball Viscometer/Densimeter (RBVD)

The equipment details of the RBVD, shown in figure 1, are summarized here and described in detail elsewhere[9, 10, 13, 15]. The RBVD, constructed from Inconel 718, has an inside diameter (ID) of 1.5875 cm and an internal volume fixed by the contraction/expansion of an internal metal bellows (BellowsTech, LLC, 1.72 cm OD). A high-pressure generator (HIP Inc., Model 37-5.75-60) delivers/removes water from the bellows that fixes the bellows position and the system pressure, as measured with two transducers (Viatran Corporation, Model 245-BMSPW, accurate to ± 0.07 MPa, for pressures to 69 MPa and Model 245-BZS, accurate to ± 0.41 MPa, for pressures to 414 MPa). The bellows position is measured with a linear, variable, differential transformer (LVDT, Schaevitz Corporation, Model 1000-HR, accurate to 0.102 mm) attached to the end of the RBVD [38, 39]. An LVDT core piece, secured to one end of a solid rod, is pulled/pushed through the sensor region of the LVDT by the rod connected to the inner face of the bellows. The RBVD cell volume is correlated to the position of the bellows through a calibration procedure described in the next section. The internal temperature of the RBVD is measured at two locations with type-K thermocouples (Omega Corporation) calibrated against a standard (Martel Electronics Corporation, BetaProbe TI+, precision to 0.01 K, accuracy to 0.06 K). For temperatures below 423 K, each location is maintained constant to within ± 0.1 K and with a temperature difference between each location within ± 0.1 K. At temperatures from 423 to 535 K, each location is maintained constant to within ± 0.2 K and with the temperature difference between each location within ± 0.2 K.

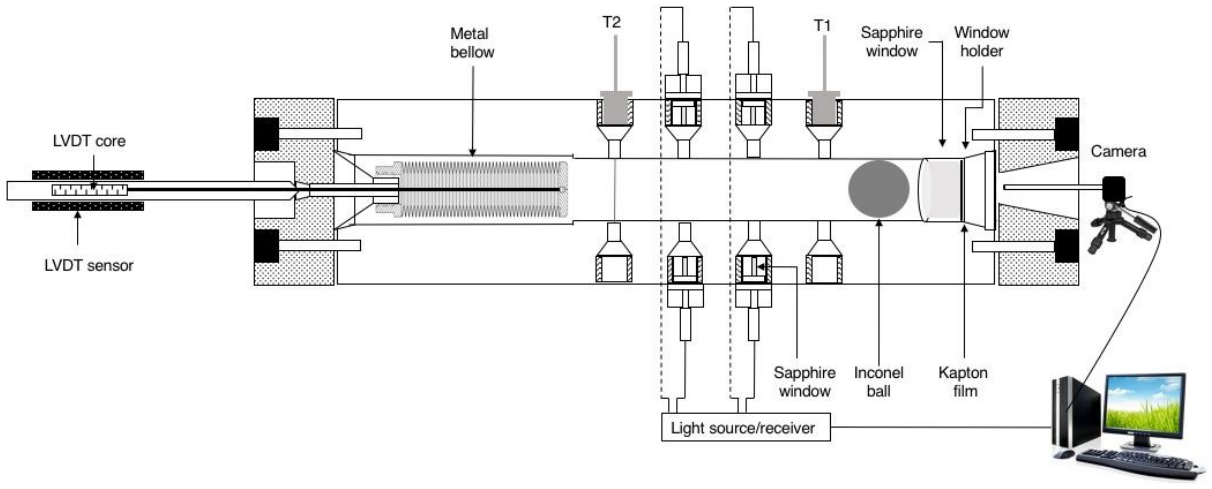

Figure 1. Schematic diagram of the windowed, rolling–ball viscometer/densimeter used in this study. T1 and T2 are thermocouples.

The ball (Industrial Tectonics Incorporated), also made of Inconel 718, has an outside diameter (OD) of 1.5796 cm, which fixes the ball OD to RBVD ID (d/D) ratio at 0.995. A borescope is positioned against the sapphire window at the front end of the RBVD to view the cell contents and to verify the ball rolls rather than slides during each measurement. A fiber optic, light transmittance-detection apparatus (Banner Engineering Corporation, sensor: Model R55FVWQ; cables: Model IF23SM900) is interfaced with a data acquisition program to measure the time, to within 0.001 s, for the ball to roll between two sets of opposing ports fitted with sapphire windows [40, 41].

2.3 RBVD Calibration

2.3.1 Density Calibration

The RBVD internal volume, V, is calibrated against the LVDT response using octane and decane density data of Caudwell et al.[3], who quote an uncertainty of 0.2% at a coverage factor, k

= 2, for both sets of data. A known mass of fluid, , *m*, to within ± 0.001, is loaded into RBVD, the temperature is fixed, and pressure is set by the bellows displacement that sets the LVDT response, x. The resultant *V*, calculated from the fluid density, is then fit to the following function

$$\mathrm{V} = \mathrm{V_0(T)}\left[1 - \ln\left(\frac{\mathrm{x} + \mathrm{B}}{\mathrm{x_0} + \mathrm{B}}\right)\right] \quad (1)$$

where x_0 is a constant related to the free-standing position of the bellows and B is a constant. V_0, the internal volume of the cell at 0.1 MPa, is set to a linear function of temperature, T.

$$\mathrm{V_0(T)} = \mathrm{v_1 T} + \mathrm{v_0} \quad (2)$$

where v_1 and v_0 are constants. The constants v_1, v_0, and B are determined using a non-linear, optimization routine that minimizes the absolute average deviation, Δ_{AAD} (equation 3), constrains the bias, Δ_{bias} (equation 5), to zero and the maximum deviation, Δ_{max} (equation 6), to a value of 0.2% reflecting the uncertainty of the density data of Caudwell et al.[3] The optimized parameters result in a $\Delta_{\mathrm{AAD}} = 0.14\%$, a standard deviation, $\Delta_{\mathrm{stdev}} = 0.08\%$ (equation 4), $\Delta_{\mathrm{bias}} = 0.00\%$, and $\Delta_{\mathrm{max}} = 0.38\%$. The Supplemental Information shows deviation graphs for the volume calculated with equations 1 and 2. The combined expanded uncertainty in the experimental densities, $U_{\mathrm{c}}(\rho)$, calculated by applying the law of error propagation, is 0.6% of the measured density value, with a coverage factor, $k = 2$.

$$\Delta_{AAD}/\% = 100 \cdot \frac{1}{N}\sum_{i=1}^{N}\left|\left(\frac{x_{i,exp} - x_{i,cal}}{x_{i,exp}}\right)\right| \quad (3)$$

$$\Delta_{stdev}/\% = \sqrt{\frac{\sum_{i=1}^{n}(\Delta_i - \Delta_{AAD})}{n-1}} \quad (4)$$

$$\Delta_{max}\Big/\% = Max\left(100 \cdot \left(\left|\frac{x_{i,exp} - x_{i,cal}}{x_{i,exp}}\right|\right)\right) \quad (5)$$

$$\Delta_{bias}/\% = \frac{1}{N}\sum_{i=1}^{N} 100 \cdot \left(\frac{x_{i,exp} - x_{i,cal}}{x_{i,exp}}\right) \quad (6)$$

where $x_{i,exp}$ and $x_{i,cal}$ are experimental and calculated data points, N is the total number of data points, and $\Delta_i = | x_{i,exp} - x_{i,cal}|$.

2.3.2 Viscosity Calibration

The working equation for the calibration parameter, K, of the RBVD is

$$K = \frac{\eta}{t \cdot (\Delta\rho) sin\theta} \quad (7)$$

where K has units of ($cm^2 \bullet s^{-2}$), η is viscosity (mPa•s), t is the ball roll time, $\Delta\rho$ ($g \bullet cm^{-3}$) is the difference between the ball and fluid densities, (ρ_b - ρ_{fl}), and θ is the RBVD angle of inclination. Hubbard and Brown[42] use a dimensional analysis technique to determine the variation of K with respect to the diameter of the ball, d_b, and tube, D_t. Lewis[43] subsequently derived an expression relating the dependency of the ratio, d_b/D_t, on K, although both expressions are valid only at ambient pressure. When operating at elevated temperatures and pressures, d_b and D_t will both vary due to effects of thermal expansion and isothermal compression. Typically the viscosities of a

reference fluid are used to determine K values that are subsequently fit to a polynomial in pressure while neglecting the weak temperature dependency of K[10, 13]. As previously mentioned, this polynomial approach requires a calibration fluid with a viscosity profile over the entire T-p region, similar to that expected for the fluid of interest.

Tomida et al.[16] and Paredes et al.[11] forgo this polynomial curve fitting method by calculating K at any T- p condition with the equation of Izuchi and Nishibata[44] (equation 7), which uses RBVD material property information to relate the ratio of K, at T and p, to K_0, at a reference T_0 and p_0.

$$K/K_0 = \left(1 + \left(\beta_b + \left(\frac{r}{1+r} - \frac{5\ r}{21-r}\right)(\beta_b - \beta_t)\right)(T - T_0) - \left(\kappa_b + \left(\frac{r}{1+r} - \frac{5\ r}{21-r}\right)(\kappa_b - \kappa_t)(p - p_0)\right)\right) \quad (8)$$

where β_b and β_t are the coefficients of thermal expansion for the ball and tube, respectively, r is equal to d_{b0}/D_{t0} determined at a reference temperature, T_0, and pressure, p_0, and κ_b and κ_t are the linear compressibility of the ball and tube, respectively. Tomida et al.[16] and Paredes et al.[11] demonstrate that the pressure effect on K can be minimized and/or neglected when the ball rolls through a tube inserted in the body of the viscometer since the tube only experiences a very small differential pressure. Conversely, our previous studies[10, 13] and the study of Sato et al.[14] clearly demonstrate a significant pressure dependency on K using a rolling ball viscometer without a tube insert. Further, Sato et al.[14] and Baled[9] show that the equation of Izuchi and Nishibata does not accurately represent the effect of pressure on K. It is worth noting that the calibration equation proposed by Izuchi and Nishibata incorporates the relationship of Lewis[43] that, unfortunately, neglects higher order terms of $[1–(d_b/D_t)]$.

Equation 9 shows the general form of our single RBVD calibration equation applicable over a wide *T*-*p* region and viscosity range and valid for a pure fluid or a complex, multicomponent mixture.

$$\frac{K}{K_0} = 1 + f(T) + g(p) \tag{9}$$

The first step is to determine a correlation for K_0 that only depends on the grouping of measurable RBVD quantities, which should be $[t\cdot(\rho_b-\rho_{fl})\cdot\sin\theta]$, as suggested by the equation for K_0 (equation 7). Normal (octane, decane, and HXD) and branched (HMN and squalane) alkane viscosity data are used to generate K_0 values as a function of p since these fluids exhibit a wide range of viscosities from ~ 1 to 1,200 cP. Figures 2(a) and 2(b) show the experimentally determined variation of $[t\cdot(\rho_b-\rho_{fl})\cdot\sin\theta]$ with pressure at 298 K for the n-alkanes and the branched alkanes, respectively. A value for $[t\cdot(\rho_b-\rho_{fl})\cdot\sin\theta]$ at 0.1 MPa can then be easily determined by extrapolating the linear curves in figure 2a for the n-alkanes. K_0 can then be readily calculated using equation 7 with viscosity data at 298 K and 0.1 MPa. However, this extrapolation is problematic for HMN and squalane given the nonlinear response of $[t\cdot(\rho_b-\rho_{fl})\cdot\sin\theta]$ to pressure shown in figure 2b.

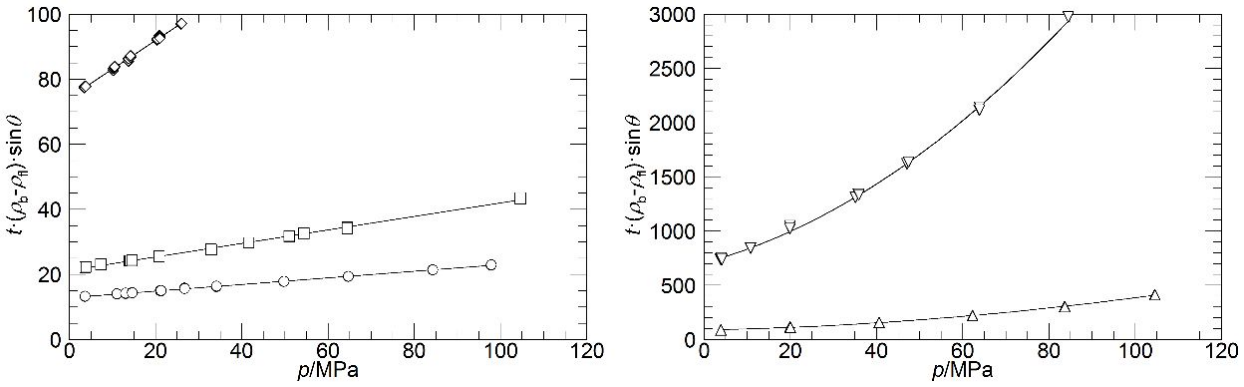

(a) (b)

Figure 2. Effect of pressure on $[t\cdot(\rho_b-\rho_{fl})\cdot\sin\theta]$ for (a) n-alkanes, ○ - n-octane, □ - n-decane, and ◇ - n-hexadecane (HXD), and for (b) branched alkanes △ - 2,2,4,4,6,8,8-heptamethylnonane (HMN), and ▽ - 2,6,10,15,19,23-hexamethyltetracosane (squalane) obtained in the present study at 298 K.

An accurate value for K_0 is needed to scale the calibration equation to the fluid of interest. However, the scaling factor $[t\cdot(\rho_b-\rho_{fl})\cdot\sin\theta]$ is only weakly dependent on fluid density since the Inconel ball density is more than an order of magnitude larger than typical hydrocarbon fluid densities. Hence, this grouping does not provide a strong signature for the fluid of interest. Bair and Yamaguchi[45] demonstrate that fluid viscosity should scale with ρ^{-n}, where n varies from 3 to 4. Figure 3a shows a new, experimentally-measured scaling factor, $[\rho_{fl}^{-3.36}\bullet\ln[t\cdot(\rho_b-\rho_{fl})\cdot\sin\theta]]$,that varies linearly with pressure for the three normal and two branched alkanes. Values of $[t\cdot(\rho_b-\rho_{fl})\cdot\sin\theta]$ at 298 K and 0.1 MPa are now reliably calculated from their respective $[\rho_{fl}^{-3.36}\cdot\ln[t\cdot(\rho_b-\rho_{fl})\cdot\sin\theta]]$ linear fit to pressure. Table 2 lists alkane K_0 (298.3 K, 0.1 MPa) values calculated using extrapolated values for $[\rho_{fl}^{-3.36}\cdot\ln[t\cdot(\rho_b-\rho_{fl})\cdot\sin\theta]]$ and literature densities and viscosities used to calculate K_0. Figure 3b shows that $-\ln[K_0]$ is related linearly to $[\rho_{fl}^{-3.36}\cdot\ln(t\cdot(\rho_b-\rho_{fl})\cdot\sin\theta)]^{-1}$ (298

K, 0.1 MPa). Therefore, for a fluid or fluid mixture of unknown ambient density and viscosity, K_0 is calculated by

1) performing RBVD measurements at 298 K and several pressures;

2) regressing $[\rho_{fl}^{-3.36}\cdot\ln(t\cdot(\rho_b-\rho_{fl})\cdot\sin\theta)]^{-1}$ to a linear curve in pressure;

3) extrapolating the curve in step 2 to 0.1 MPa to obtain a value for $[\rho_{fl}^{-3.36}\cdot\ln(t\cdot(\rho_b-\rho_{fl})\cdot\sin\theta)]^{-1}$ at 298 K

4) substituting the extrapolated value into equation 10.

The results listed in table 2 show that calculated K_0 values using equation 10 are in good agreement with experimental values as indicated by a Δ_{AAD} = 0.38%, Δ_{stdev} =0.32% , Δ_{bias} = 0%, and a Δ_{max} = 0.65%.

$$K_0 = e^{-[mx+b]} \tag{10}$$

where x = $[\rho_{fl}^{-3.36}\cdot\ln(t\cdot(\rho_b-\rho_{fl})\cdot\sin\theta)]^{-1}$ (298 K, 0.1 MPa), m = 1.8938, and b = 7.6163.

As previously mentioned, the ball is made of Inconel 718, the same metal as the RBVD body to minimize the effect of temperature on K. Although the ratio d_b/D_t is unaffected by thermal expansion, the calibration equation derived by Hubbard and Brown[42] does contain the term $d_b(d_b+D_b)$, which will vary with temperature. Here we use the expression recommended by Sato et al.[14] to account for the effect of temperature on K.

$$f(T) = 2\beta(T - T_0) \tag{11}$$

where β is the coefficient of thermal expansion of Inconel 718[46], the RBVD material of construction.

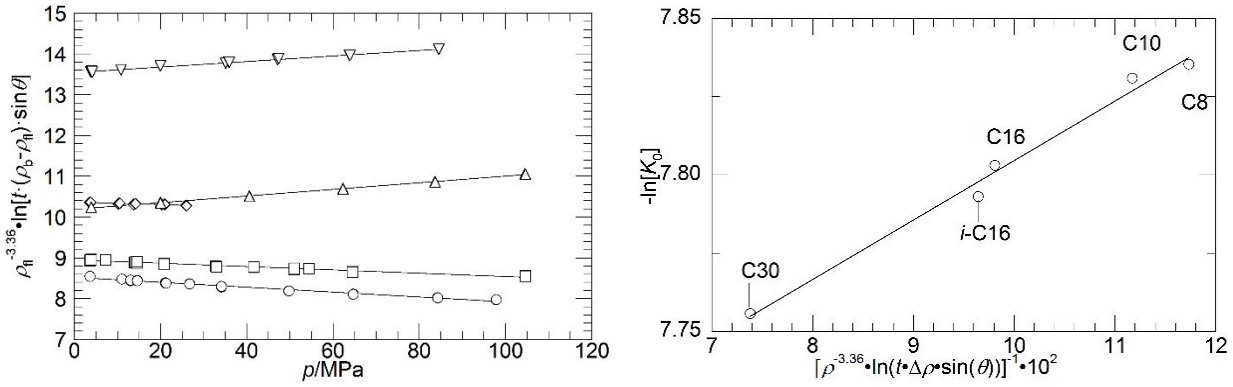

(a) (b)

Figure 3. (a) Linear response of $[\rho_{fl}^{-3.36}\cdot\ln[t\cdot(\rho_b-\rho_{fl})\cdot\sin\theta]]$ to pressure at 298 K obtained in this study for ○ - n-octane, □ - n-decane, ◇ - n-hexadecane (HXD), △ - 2,2,4,4,6,8,8-heptamethylnonane (HMN), and ▽ - 2,6,10,15,19,23-hexamethyltetracosane (squalane). (b) Correlation of K_0 with $[\rho_{fl}^{-3.36}\cdot\ln[t\cdot(\rho_b-\rho_{fl})\cdot\sin\theta]]^{-1}$ at 298 K and 0.1 MPa where $\Delta\rho = (\rho_b-\rho_{fl})$, C8 - n-octane, C10 - n-decane, C16 - n-hexadecane, *i*-C16 - 2,2,4,4,6,8,8-heptamethylnonane, and C30 - 2,6,10,15,19,23-hexamethyltetracosane.

Table 2. K_0 coefficients determined at 298.3 K and 0.1 MPa for n-octane, n-decane, n-hexadecane (HXD), 2,2,4,4,6,8,8-heptamethylnonane (HMN), and 2,6,10,15,19,23-hexamethyltetracosane (squalane) listed with the literature source for ρ, the uncertainty of ρ, $U_c(\rho)$, the literature source for η, and the uncertainty of η, $U_c(\eta)$.

Fluid	$K_0 \cdot 10^4$ /cm·s^{-2}	Source of ρ	$U_c(\rho)$ (%)	Source of η	$U_c(\eta)$ (%)
n-octane	3.969	Wu et al.[47]	0.02	Knapstad et al.[48]	0.33
n-decane	3.987	Wu et al.[47]	0.02	Knapstad et al.[48]	0.33
HXD	4.130	Wu et al.[47]	0.02	Wu et al.[47]	0.1
HMN	4.084	Et Tahir et al.[32]	0.03	Et Tahir et al. [32]	1.0
squalane	4.312	Harris et al.[8]	0.05	Mylona et al. [30]	1.5

Equation 12 is used to determine values for $g(p)$, the pressure effect on K/K_0, that are plotted in figure 4 for octane data of Caudwell[3]. Similar results are obtained for decane although these data are not shown to minimize clutter in the graph. Equation 13 is proposed to account for the pressure effect on K/K_0, where K is experimentally determined using highly accurate literature viscosity data for n-octane to 473 K and 200 MPa and n-decane to 348 K and 200 MPa.[3] K_0 is calculated as previously described. When C, D, and E are fixed constants, equation 13 has a Δ_{AAD} = 0.97%, Δ_{stdev} = 1.04%, Δ_{bias} = 0%, and Δ_{max} = 5.27% and 94% of the data are within 2.5% of calculated values. However, systematic deviations are observed at the highest pressures at the temperature extremes of 298 and 473 K. Therefore, C, D, and E are refit but now allowed to vary with temperature as shown in equations 14 to 16, respectively. The K/K_0 deviation plots, figures 5(a) and 5(b), exhibit only a small amount of systematic deviations at 298 and 473 K. In this case

the Δ_{AAD} = 0.84%, Δ_{stdev} =0.70%, Δ_{bias} = 0.16%, and Δ_{max} = 3.05% and 97% of the data are within 2.5%. The temperature correction for C, D and E may be attributed to the subtle effect of temperature on the compressibility of the Inconel 718[46].

$$g(p) = \frac{K}{K_0} - 1 - 2\beta(T - T_0) \quad (12)$$

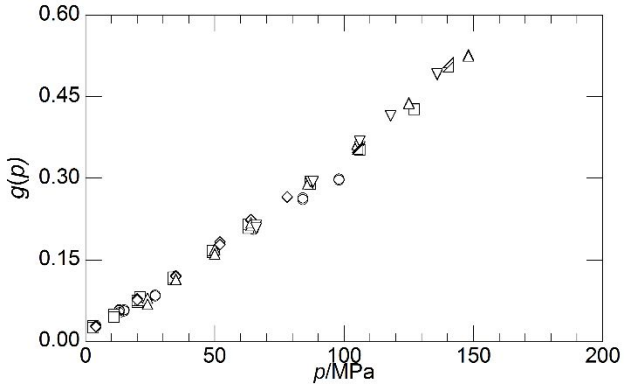

Figure 4. Effect of pressure on $g(p)$, the pressure correction term for K/K_0 determined experimentally with octane data of Caudwell et al.[3] ○ - 298.4, □ - 326.5, ◇ - 347.4, △ - 375.5, ▽ - 422.2, and ◿ - 470.3.

$$g(p) = C\left[ln\left(\frac{p}{p_0}\right)\right]\left(\frac{D + p}{D + p_0}\right)^E \quad (13)$$

$$C = c_1 T + c_0 \quad (14)$$

$$D = d_1 T + d_0 \quad (15)$$

$$E = e_1 T^{-1} + e_0 \quad (16)$$

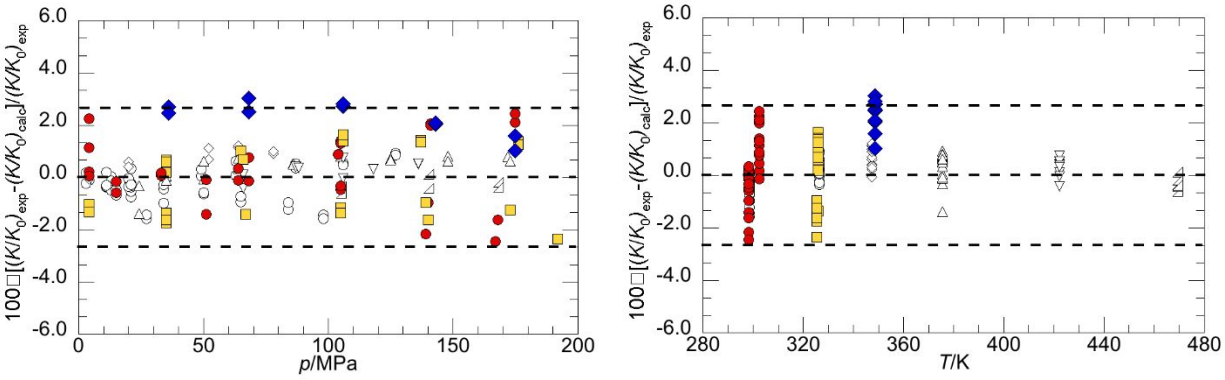

Figure 5. Comparison of experimentally determined calibration parameters, $(K/K_0)_{exp}$, to calculated parameters, $(K/K_0)_{calc}$, accounting for the effect of temperature on the parameters in the equation for $g(p)$. ○ - 298.4, □ - 326.5, ◇ - 347.4 , △ - 375.5 , ▽ - 422.2, ◿ - 470.3, ● - 302.5 K, ■ - 325.9, and ◆ - 348.7 K where open and filled symbols represent octane and decane, respectively. Lines at ± 2.5% reflect the combined expanded uncertainty for K, where $U_c(K) = 0.025 \bullet K$. **Note that many data points superpose in these graphs.**

The final calibration equation for the RBVD utilized in our study is,

$$\frac{K}{K_0} = 1 + 2\beta(T - T_0) + C\left[\ln\left(\frac{p}{p_0}\right)\right]\left(\frac{D + p}{D + p_0}\right)^E \qquad (17)$$

The combined expanded uncertainty of K, $U_c(K)$, is 2.5%, with a coverage factor, $k = 2$, as determined by applying the law of error propagation to equation 16 and using the uncertainties for the measured RBVD experimental quantities, $u(T) = 0.1$ K at $T < 422$ K and 0.2 K at $T > 422$ K, and $u(p) = 0.07$ MPa at $p \leq 68.9$ MPa and 0.41 MPa at $p > 68.9$ MPa, $u(t) = 0.001$s, and $u(\theta) = 0.016^o$. The combined expanded uncertainty in the viscosity is $U_c(\eta) = 0.025 \bullet \eta$ mPa•s with a coverage factor, k = 2.

3. Experimental Results

3.1 Density Comparisons

The Supplemental Information (SI) lists tables for the densities and viscosities for HXD, squalane, and HMN obtained in this study from 300 to 530 K and to pressures of 250 MPa. The SI shows *p*-*T* plots of available literature data for these compounds and highlights were original data are obtained in the present study. Densities obtained in this study are validated against experimental data and available reference correlations. The reference correlation of Romeo and Lemmon[49] is used for HXD and the reference correlation of Mylona et al.[19] is used for squalane. Both reference correlations were regressed against highly accurate, primary, experimental data and they accurately represent these data over a large *T*-*p* region. To the best of our knowledge there are no reference correlations for HMN and, therefore, the HMN data from the present study are fit to the Tait equation to facilitate comparison to available literature data.

3.1.1 EoS of Romeo and Lemmon[49] (HXD)

Romeo and Lemmon[49] provide an equation of state (RL-EoS) for HXD covering the *T*-*p* region from the triple point to 800 K and pressures to 50 MPa. In addition, Meng et al.[18] shows that extrapolating the RL-EoS to 300 MPa provides predictions within 0.5% of available literature densities. Figures 6(a) and 6(b) show comparisons of experimental densities obtained in the present study, those from other studies, and those calculated using the RL-EoS. All of the data from the present study are within ± 0.6% of the densities calculated with the RL-EoS. The HXD density data from the present study are in excellent agreement with RL-EoS calculated densities as noted by an $\Delta_{AAD} = 0.21\%$, $\Delta_{stdev} = 0.15\%$, $\Delta_{max} = 0.46\%$, and $\Delta_{bias} = -0.19\%$.

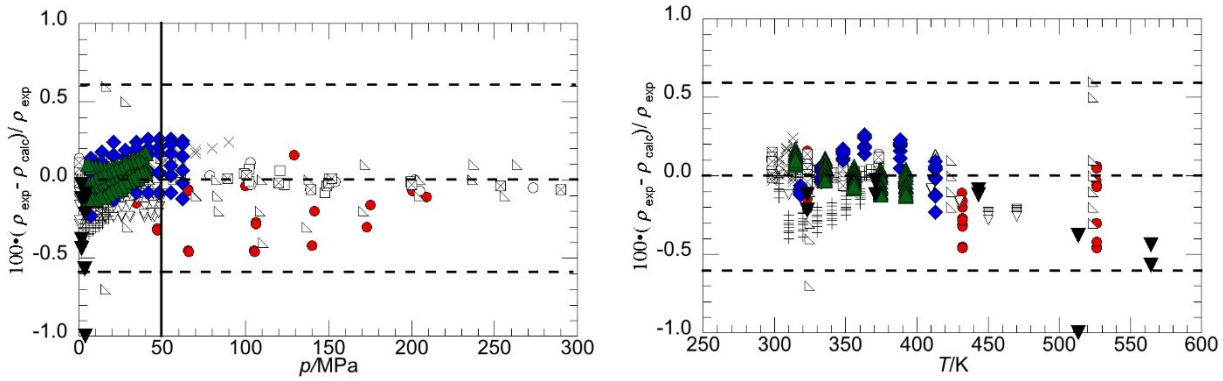

(a) (b)

Figure 6. Comparisons of experimental n-hexadecane (HXD) densities, ρ_{exp}, obtained in the present study and other studies to calculated densities, ρ_{calc}, using the Romeo and Lemmon equation of state (RL-EoS)[49]. ● - this study, ○ - Dymond et al. (1980)[50], □ - Tanaka et al.[51], ◇ - Kleinschmidt et al.[52], △ - Chang et al.[53], ▽ - Outcault et al.[54], ◿ - Wu et al.[39], ⊞ - Banipal et al.[55], ⊠ - Dymond et al. (1979)[56], + - Glaser et al.[57], × - Wurflinger et al.[58], ◆ - Amorim et al.[59], ▲ - Gouel et al.[60], and ▼ - Matthews et al.[61]. The solid vertical black line drawn at 50 MPa represents the pressure limit imposed on the RL-EoS. Horizontal dashed lines at ± 0.6% reflect the combined expanded uncertainty for density obtained in the present study where, $U_c(\rho) = 0.006 \bullet \rho$, with a coverage factor, k = 2. **Note that many data points superpose in these graphs.**

3.1.2 Reference Correlation of Mylona et al.[19] (squalane)

Mylona et al.[19] provide a reference correlation for squalane density covering the *T*-*p* region from 273 to 473 K and pressures up to 200 MPa. Figures 7(a) and 7(b) show comparisons of experimental densities obtained in the present study, those from other studies, and those calculated using using the reference correlation of Mylona et al. The squalane density data from the present

study are in excellent agreement with the densities calculated using the reference correlation of Mylona et al. as noted by an $\Delta_{AAD} = 0.33\%$, $\Delta_{stdev} = 0.25\%$, $\Delta_{max} = 0.95\%$, and $\Delta_{bias} = -0.04\,\%$.

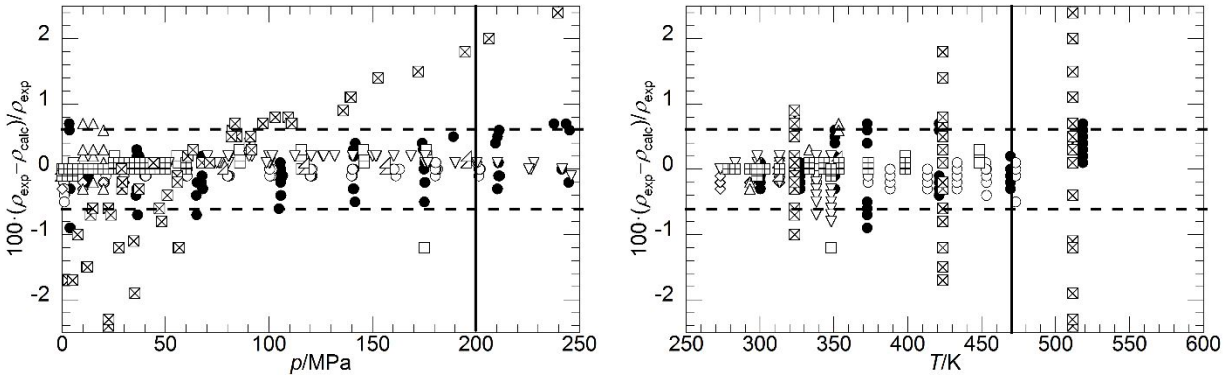

(a) (b)

Figure 7. Comparisons of experimental 2,6,10,15,19,23-hexamethyltetracosane (squalane) densities, ρ_{exp}, obtained in the present study and other studies to calculated densities, ρ_{calc}, using the reference correlation of Mylona et al.[19]. ● - This study, ○ - Schmidt[6], □ - Ciotta[4], ◇ - Kumagai[28], △ - Tomida[16], ▽ - Harris[8], ◿ - Kuss and Golly[62], ⊞ - Fandino et al. (2005 & 2010)[24, 25], and ⊠ - Bamgbade et al.[23]. The solid vertical black lines drawn at 200 MPa in (a) and 473 K in (b) reflect the pressure and temperature limits of the reference correlation, respectively. Dashed lines at ± 0.6% reflect the combined expanded uncertainty for densities obtained in the present study where, $U_c(\rho) = 0.006 \bullet \rho$, with a coverage factor, k = 2.

3.1.3 Tait Equation for HMN Densities

Density data for HMN from this study are fit to the Tait equation for facile interpolation and ease of comparison to available literature data given that, to the best of our knowledge, a primary HMN reference correlation has not been reported in the literature. The fitting procedure

is described by Caudwell et al.[3] and in our previous studies [13, 39] and further details are found in the SI. Figures 8(a) and 8(b) show that all of the densities reported in the present study and, in fact, all of the available literature data agree to within our combined expanded uncertainty of 0.6%. The overall level of agreement of the data from the present study to the densities calculated with the Tait equation is summarized by a $\Delta_{AAD} = 0.07\%$, $\Delta_{stdev} = 0.09\%$, $\Delta_{max} = 0.39\%$, and $\Delta_{bias} = 0.00\%$.

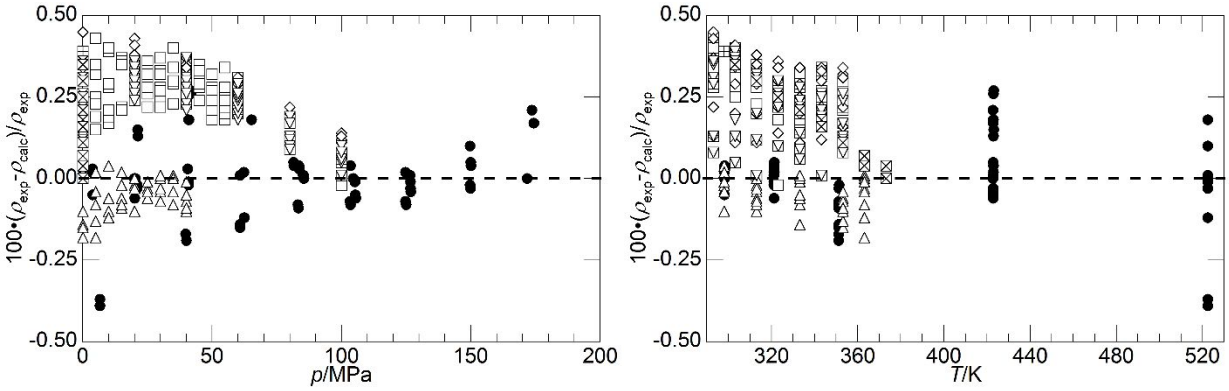

(a) (b)

Figure 8. Comparison of experimental 2,2,4,4,6,8,8-heptamethylnonane (HMN) densities, ρ_{exp}, obtained in the present study and other studies to Tait calculated densities, ρ_{calc}. ● - This study, □ - Cannet et al.[31], ◇ - Barrahou et al.[63], △ - Et-Tahir et al.[32], ▽ - Zeberg-Mikkelsen et al.[37], ⊞ - Fermeglia and Torriano[33], and ⊠ - Lunning-Prak et al.[36, 64, 65].

3.2. Viscosity Comparisons

Meng et al.[18] report a viscosity reference correlation for HXD and Mylona et al.[19] report a viscosity reference correlation for squalane. The correlations for both compounds used here are regressed to primary experimental data and accurately represent data over a large *T*-*p* region. Huber[66] provides a preliminary viscosity model for HMN, however, this model is not applicable to the range of conditions covered in this study. Hence, the HMN viscosity data reported in the

present study are fit to a modified Tait equation and then compared to available literature data. The last section shows a direct comparison of HXD, HMN, and squalane viscosities obtained in the present study using the universal calibration method to determine K and using a simple quadratic polynomial to determine K.

3.2.1 Reference Correlation of Meng et al.[18] (HXD)

The viscosity reference correlation of Meng et al. is a function of temperature and density where the density is calculated with the RL-EoS. Meng et al. report an estimated uncertainty of 2.5% with a coverage factor, $k = 2$ for viscosities calculated from 298 to 373 K and to 200 MPa and from 373 to 473 K and to 100 MPa. Figures 9(a) and 9(b) show comparisons of HXD viscosities obtained in this study using the K/K_0 calibration equation, viscosities obtained from the literature, and viscosities calculated from the reference correlation. In this instance there is very good agreement between viscosities from the present study to those calculated with the correlation. Note that 91% of the HXD viscosity data obtained in the present study are within the uncertainty of the reference correlation.

Meng et al. report a second reference correlation that has a larger estimated uncertainty of 5% for viscosities calculated from 373 to 473 K and 100 to 200 MPa, and from 473 to 675 K and 4 to 200 MPa. The larger uncertainty is attributed to the lack of primary experimental data needed to fine tune the correlation in these two T-p regions. Figures 10(a) and 10(b) show that 76% of the HXD viscosity data obtained in the present study are within ± 5%, the estimated uncertainty of the reference correlation.

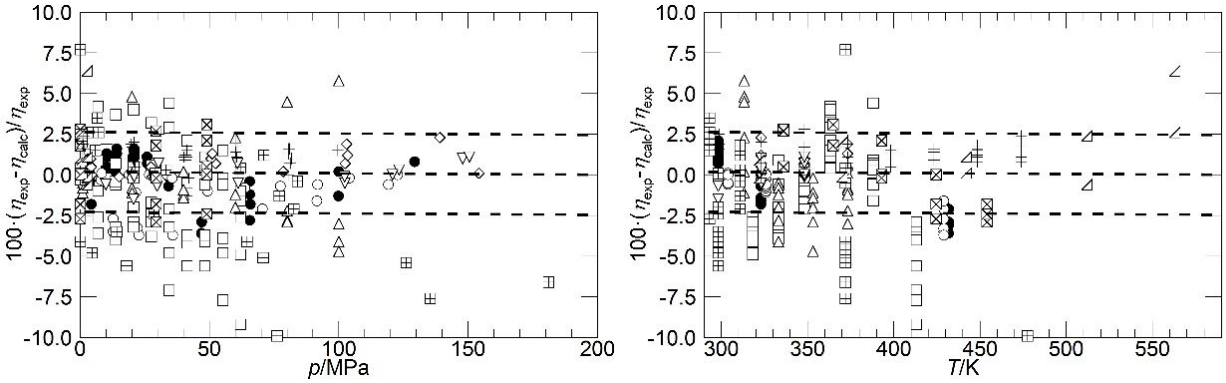

(a) (b)

Figure 9. Comparisons of experimental n-hexadecane (HXD) viscosities, η_{exp}, obtained in the present study and in other studies to calculated viscosities, η_{calc}, with the reference correlation of Meng et al.[18]. The comparisons are limited within the *T*-*p* regions from 298 to 373 K and pressures to 200 MPa, and from 373 to 473 K and pressures to 100 MPa, where the uncertainty of the reference correlation in both regions is 2.5% with a coverage factor, $k = 2$. ● - This study, ○ - Baled et al.[10], □ - Rajagopal et al.[67], △ - Ducoulombier et al.[68], ◇ - Dymond et al.[50], ▽ - Tanaka et al.[51], ⊞ - Kleinschmidt et al.[52], ⊠ - Rastogorev et al.[69], ⊿ - Matthews et al.[61], and ＋ - Mohammad et al.[70]. Dashed lines are drawn at ± 2.5% to reflect the uncertainty of the reference correlation of Meng et al.

3.2.2 Reference Correlations of Mylona et al.[19] (squalane)

Mylona and co-workers report two squalane reference viscosity correlations, $\eta_{ref}(T, \rho)$ and $\eta_{ref}(T, p)$, described in detail elsewhere[19]. The $\eta_{ref}(T, \rho)$ correlation is limited to 323 to 473 K and pressures to 200 MPa, and has an estimated uncertainty of 3% with a coverage factor, k = 2. Figures 11(a) and 11(b) show comparisons of squalane viscosities obtained in this study using the K/K_0 calibration equation, viscosities obtained from the literature, and viscosities calculated with the $\eta_{ref}(T, \rho)$ correlation. In this instance there is excellent agreement between the squalane viscosities

measured in this study to those calculated with the correlation of Mylona et al. Note that 94% of the squalane viscosity data obtained in the present study are within the 3% estimated uncertainty of the reference correlation.

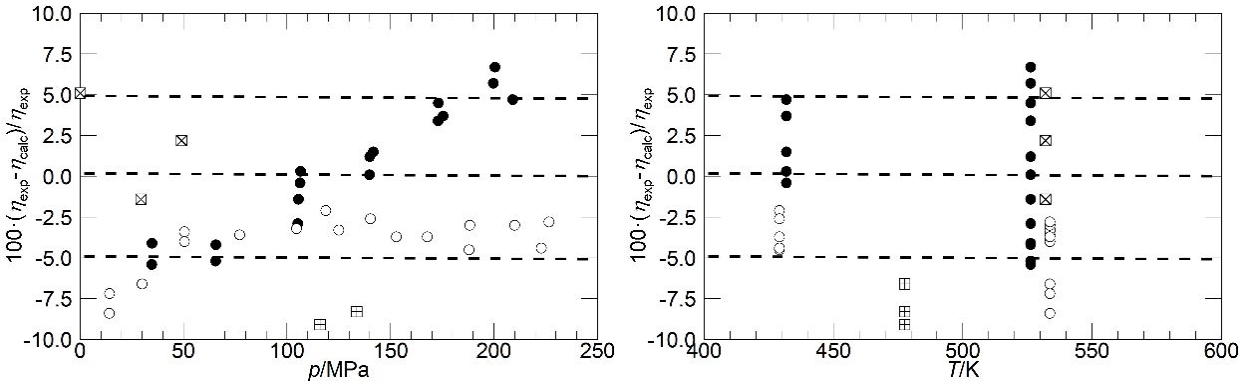

(a) (b)

Figure 10. Comparisons of experimental n-hexadecane (HXD) viscosities, $\eta_{exp,}$ obtained in the present study and in other studies to calculated viscosities, η_{calc}, using the reference correlation of Meng et al.[18]. The comparisons are limited within the *T*-*p* regions from 373 to 473 K and pressures from 100 to 200 MPa and from 473 to 675 K and pressures from 4 to 200 MPa, where the uncertainty of the reference correlation in these regions is 5% with a coverage factor, $k = 2$. ● - This study, ○ - Baled et al.[10], ⊞ - Kleinschmidt et al.[52], and ⊠ - Rastogorev et al.[69] Dashed lines are drawn at ± 5% reflecting the estimated uncertainty of the reference correlation of Meng et al.

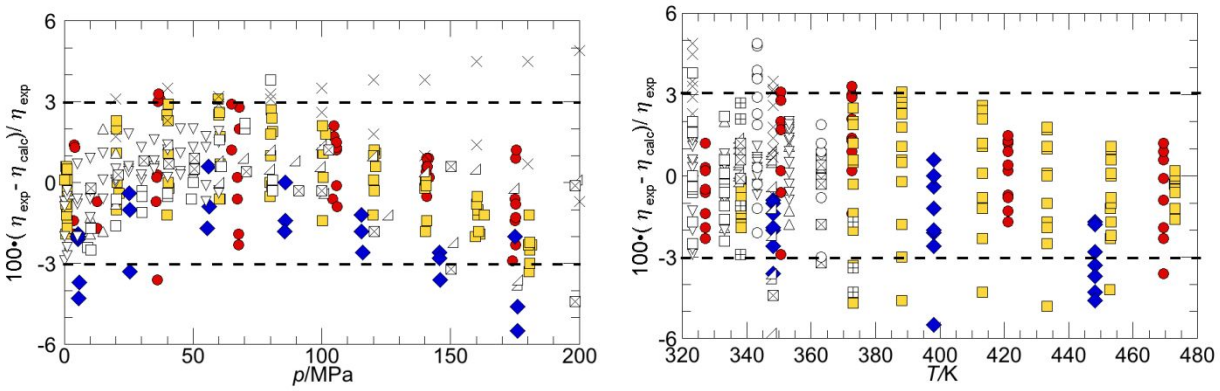

Figure 11. Comparisons of experimental 2,6,10,15,19,23-hexamethyltetracosane (squalane) viscosities, η_{exp}, obtained in the present study and in other studies to calculated viscosities, η_{calc}, using the $\eta_{ref}(T, \rho)$ reference correlation of Mylona et al.[19]. ● - This study, ■ - Schmidt et al.[6], ◆ - Ciotta et al.[4], △ - Tomida et al.[16], ▽ - Pensado et al.[12], ◿ - Harris[8], ⊠ - Comuñas-FB-UNSW[71], ○ - Comuñas-FB-UPPA[71], □ - Comuñas QCR[71]. Lines drawn at ± 3% reflect the estimated uncertainty of the reference correlation.

The $\eta_{ref}(T, p)$ correlation by Mylona and co-workers[19] covers a wider range of conditions from 273 to 473 K and pressures to 200 MPa, but has a larger estimated uncertainty of 4.75% with a coverage factor, k = 2. Figures 12(a) and 12(b) show comparisons of squalane viscosities obtained in this study using the K/K_0 calibration equation, viscosities obtained from the literature, and viscosities calculated with the $\eta_{ref}(T, p)$ correlation. In this instance 87% of the squalane viscosity data are within ± 4.75% again reflecting very reasonable agreement between the data obtained in this study and an accepted correlation.

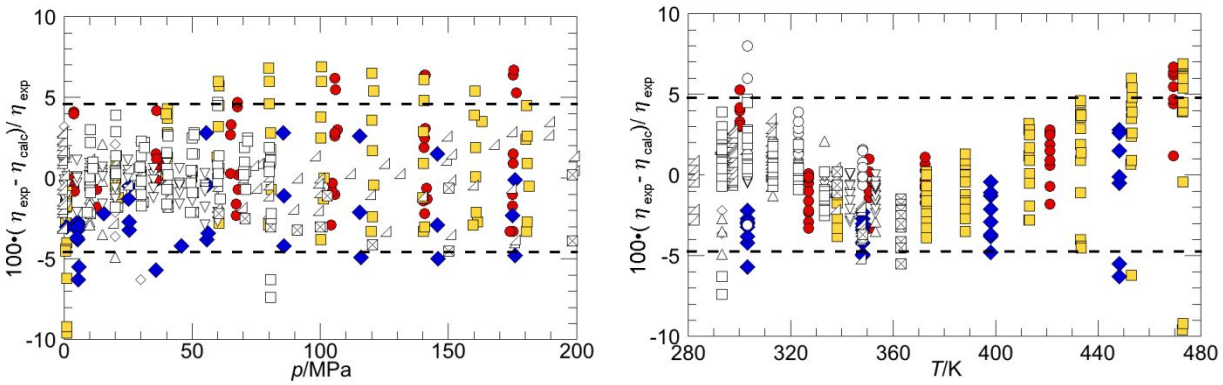

(a) (b)

Figure 12. Comparisons of experimental 2,6,10,15,19,23-hexamethyltetracosane (squalane) viscosities, η_{exp}, obtained in the present study and in other studies to calculated viscosities, η_{calc}, using the $\eta_{ref}(T, p)$ reference correlation of Mylona et al.[19] ● - This study, ■ - Schmidt et al.[6], ◆ - Ciotta et al.[4], ◇ - Kumagai et al.[28], △ - Tomida et al.[16], ▽ - Pensado et al.[12], ◿ - Harris[8], ⊠ - Comuñas-FB-UNSW[71], ○ - Comuñas-FB-UPPA[71], □ - Comuñas QCR[71]. Lines drawn at ± 4.75% reflect the estimated uncertainty of the reference correlation.

3.2.3 Comparison to Viscosity Literature Data for HMN

HMN viscosity data from the present study are fit to a modified Tait equation for facile interpolation and ease of comparison to available literature data. The fitting procedure is described by Caudwell et al.[3] and in our previous studies [13, 39] and further details are found in the Supplemental Information. At temperatures up to 353 K the Tait equation is used up to pressures of 150 MPa and at temperatures greater than 353 K the equation is used to pressures of 200 MPa, which are *T*-*p* ranges that closely match the conditions where viscosity data are obtained in the present study. In these specific *T*-*p* ranges the fit of the Tait equation has a Δ_{AAD} = 1.0%, Δ_{stdev} = 0.09%, Δ_{bias} = 0.0%, Δ_{max} = 3.5, and 96% of the data are within ± 2.5% of calculated values.

Figures 13(a) and 13(b) show comparisons of HMN viscosities obtained in this study using the K/K_0 calibration equation, viscosities obtained from the literature, and viscosities calculated with the modified Tait equation. The measurements of Bair at 313 and 373 K to 150 MPa, with the exception of one data point at 0.1 MPa, compare to our calculated Tait viscosities to within 2.5%. Note that the data reported by Fermeglia and Torriano[33] and Lunning-Prak et al.[36, 64, 65] are limited to ambient pressure and these literature data exhibit consistently negative deviations ranging from 2.5 to 5%. These large deviations are not unexpected considering that ambient pressure data were not obtained in the present study and, hence, not accounted for with the Tait equation used to interpolate our data. The viscosity data reported by Krahn and Luft[27] agree within 5% to data from the present study at 298 and 353 K and pressures only up to 120 MPa, which is the maximum pressure obtained in the present study at these two temperatures. However, with the exception of one data point at 50 MPa, the 453 K data of Krahn and Luft agree within 1.6% of the data obtained in the present study for pressures to 200 MPa.

Note that the data of Cannet et al.[31], Barrohou et al.[63], Et-Tahir et al.[32], and Zeberg-Mikkelsen et al.[63] deviate from those in the present study by as much as 11% at the lowest temperatures and highest pressures. A possible cause for these high deviations could be related to the fluid used to calibrate the falling-body viscometers used in each of these studies. Each of the viscometers were calibrated with decane, whose viscosities range from 0.4 to 2.2 mPa•s over the *T-p* region of 298 to 373 K and pressures to 100 MPa, whereas HMN viscosities are an order of magnitude higher, from 1.8 – 22 mPa•s, in approximately the same *T-p* region. It is interesting to note that a similar degree of deviation is observed for 1-methylnaphthalene viscosities measured by Caudwell et al.[3], using an absolute technique, to data of Et-Tahir et al.[32] and Cannet et al.[31] using a relative technique, but calibrated with a less viscous fluid.

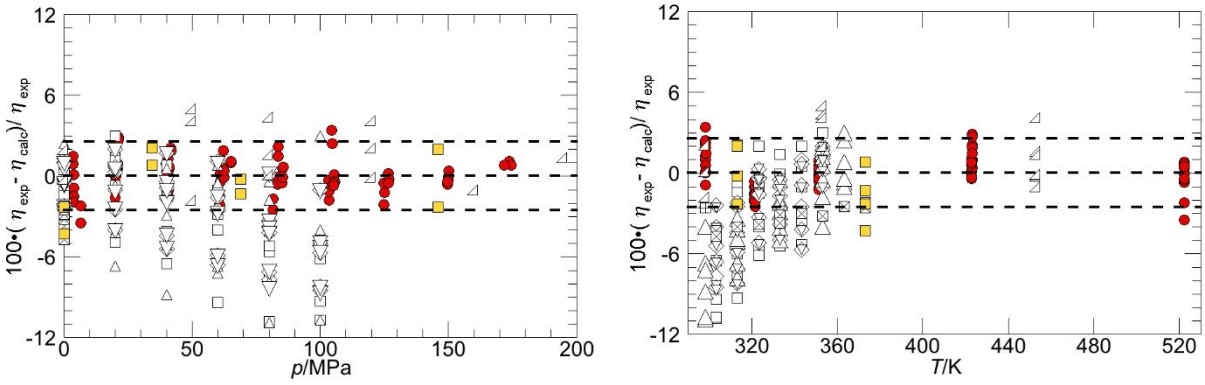

(a) (b)

Figure 13. Comparison of experimental 2,2,4,4,6,8,8-heptamethylnonane (HMN) viscosities, η_{exp}, obtained in the present study and other studies to Tait calculated viscosities, η_{calc}. ● - This study, ■ - Bair[20], □ - Cannet et al.,◇ - Barrahou et al.[63], △ - Et-Tahir et al.[32], ▽ - Zeberg-Mikkelsen et al.[37], ◿ - Krahn and Luft[27], ⊞ - Fermeglia and Torriano[33], and ⊠ - Lunning-Prak et al.[36, 64, 65]. Lines drawn ± 2.5% reflect the estimated uncertainty of the viscosities calculated with the modified Tait equation. **Note that many data points superpose in these graphs.**

3.2.4 Comparison of HXD, HMN, and Squalane Viscosities Calculated With the Universal Calibration Method and With a Quadratic Polynomial

The previous sections of the manuscript provide evidence for the reliability of the viscosity data obtained in the present study using the new, universal RBVD calibration curve. The typical alternative method to generate an RBVD calibration curve is to use reliable literature viscosity data and regress K to a quadratic polynomial in pressure. Figure 14 shows a deviation graph comparing all of the HXD, HMN, and squalane viscosities determined using the new, universal RBVD calibration curve and using a quadratic polynomial representation for K obtained using

octane and decane data of Caudwell[3] from 298 to 473 K and pressures to 200 MPa. Very large deviations, outside the estimated experimental uncertainty of our technique, are observed when octane and decane are used to generate a simple, quadratic calibration equation for *K*. As noted earlier, octane and decane viscosities are much lower than any of those exhibited by the higher molecular weight fluids shown in figure 14. Hence, the greatest deviations exhibited by squalane are not unexpected since squalane viscosities are significantly larger than octane or decane viscosities. Another notable trend is that the deviations increase most dramatically at pressures greater than 150 MPa.

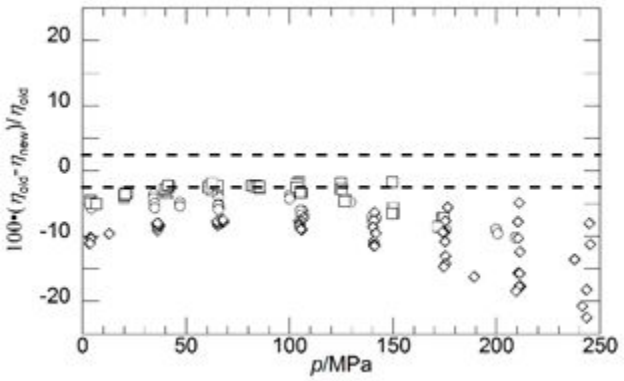

Figure 14. Comparison of all of the experimental HXD (◇), HMN (△), and squalane (▽) viscosities obtained in the present study using a quadratic polynomial to represent K, η_{old}, and using the new RBVD universal calibration curve for *K*, η_{new}. Lines drawn ± 2.5% reflect the estimated experimental uncertainty of the viscosities.

3.3 Density and Viscosity Modeling

Densities are modeled using the PC-SAFT EoS with pure component parameters calculated from the HPHT group contribution (GC) approach reported by Burgess et al.[72]. Viscosities are calculated with Free Volume Theory (FVT), where the required input densities are calculated with

the GC-PC-SAFT EoS[73]. Detailed descriptions of the viscosity calculations are found elsewhere[9, 10, 13, 15, 73].

3.3.1 Density Calculated With GC-PC-SAFT

Table 3 shows the PC-SAFT parameters m, σ, and ε/k obtained with the HTHP-GC approach reported by Burgess et al.[72]. All of the HXD calculated densities compare to experimental values within 0.6%, which is the estimated uncertainty of our data. While the majority of the HMN calculated densities agree closely with experimental values, a small portion of the calculated HMN densities at 423 and 523 K exhibit deviations as high as 1%, which is slightly outside of our estimated experimental uncertainty. In contrast, the GC-PC-SAFT EoS does a poor job matching experimental squalane densities given that deviations as high as 2.2% are observed at the lowest temperatures and highest pressures. This larger deviation is perhaps not unexpected given that Burgess et al.[72] did not include squalane data in the development of the GC parameters. (see the deviation graphs in the Supplemental Information)

Table 3. PC-SAFT parameters m, σ, and ε/k calculated using the Group Contribution method of Burgess et al.[72] for HXD, HMN, and squalane.

Fluid	m	σ	ε/k	Δ_{AAD}/%	Δ_{max}/%
HXD	10.218	3.4218	241.76	0.3	0.4
HMN	8.9687	3.5767	256.44	0.5	1.0
squalane	17.2942	3.5051	242.45	0.7	2.2

3.3.2 Viscosity Calculated With Free Volume Theory

Viscosity data are modeled using FVT, which is composed of a dilute gas viscosity, η_0 (equation 18) calculated from the kinetic theory of gases, and a residual term, $\Delta\eta$ (equation 19) given by Allal et al.[74]

$$\eta/\mathrm{mPa}\cdot\mathrm{s} = \eta_0 + \Delta\eta \tag{18}$$

$$\Delta\eta/\mathrm{mPa}\cdot\mathrm{s} = \frac{\rho L\left(\alpha\rho + \frac{pM}{\rho}\right)}{\sqrt{3RTM}}\exp\left[B_v\left(\frac{\alpha\rho + \frac{pM}{\rho}}{RT}\right)^{3/2}\right] \tag{19}$$

where ρ is calculated using the GC-PC-SAFT EoS with parameters listed in table 3, M (kg•mol^{-1}) is molecular weight, and R is the universal gas constant. Table 4 lists the three FVT parameters, L (Å), α (m^5•mol^{-1}•s^{-2}), and B_v (dimensionless), calculated from correlations reported by Polishuk and Yitzhak[75], along with statistical measures of the FVT predictions. Very reasonable Δ_{AAD} and Δ_{max} values are obtained for HXD. However, large Δ_{AAD} and Δ_{max} values are obtained for HMN and squalane, which are not unexpected since the Polishuk-Yitzhak correlation does not explicitly account for effect of branching in alkanes. It should be noted that a certain fraction of the large deviation with the branched alkanes may be attributable to the values of ρ calculated here with the GC-PC-SAFT EoS as compared to the SAFT + cubic EoS used by Polishuk and Yitzhak.

Table 5 lists calculation results when the FVT parameters are fit to viscosity data obtained in this study. The parameter values listed in table 4 are used as initial guesses while minimizing the Δ_{AAD}, constraining Δ_{bias} to zero, and constraining Δ_{max} to 5%. Little improvement is seen for HXD viscosity predictions however, for branched alkanes, HMN and squalane, deviations are each

reduced by a factor of 3 to 4. Nonetheless, in comparison to deviations exhibited by HXD, deviations for HMN are greater by roughly a factor of two and for squalane by a factor of six. The poor performance for branched relative to linear alkanes may be due to a poor representation of the free volume behavior of these two alkane structures. Yashi[76] shows that the relationship between viscosity and free volume of branched alkanes exhibit a strong temperature dependency, whereas n-alkanes do not. Further work is in progress to elucidate the underlying phenomenon of free volume relationship to viscosity

Table 4. FVT parameters L, α, and B_v are calculated using the correlation of Polishuk and Yitzhak[75] for n-hexadecane (HXD), 2,2,4,4,6,8,8-heptamethylnonane (HMN), and squalane. Densities needed for the FVT predictions are calculated with the GC-PC-SAFT EoS. The performance of FVT is characterized by the Δ_{AAD} and Δ_{max}.

Fluid	L/Å	α/m^5•mol^{-1}•s^{-2}	B_v•10^3	Δ_{AAD}/%	Δ_{max}/%
HXD	0.7733	235.97	3.6689	3.8	9.6
HMN	0.7733	235.97	3.6689	27.2	62.3
squalane	0.6478	436.26	1.7353	55.4	94.5

Table 5. FVT parameters L, α, and B_v optimized by fitting viscosity data obtained in this study for n-hexadecane (HXD), 2,2,4,4,6,8,8-heptamethylnoane (HMN), and squalane. Densities needed for the FVT predictions are calculated with the GC-PC-SAFT EoS. The performance of FVT is characterized by the Δ_{AAD} and Δ_{max}.

Fluid	L/Å	α/m^5•mol^{-1}•s^{-2}	B_v•10^3	Δ_{AAD}/%	Δ_{max}/%
HXD	0.6763	266.08	3.2313	3.1	5.2
HMN	0.6867	179.61	7.1694	6.7	12.8
squalane	0.1549	643.66	1.8693	17.5	35.3

To improve the FVT viscosity predictions, α and B_v are allowed to vary with temperature while keeping L as a constant since this parameter is expected to scale with molecular size, which should be independent of temperature. Consistent with the approach used in our previous study[13] α and B_v are fit to quadratic functions of temperature, equations 20 and 21, respectively. Table 6 lists the parameters needed for the FVT calculations using temperature-dependent parameters along with Δ_{AAD} and Δ_{max} values that characterize the FVT fit of the data. The performance of FVT is significantly improved by making both parameters α and B_v temperature dependent, especially for the branched alkane viscosities.

$$\alpha/m^5 \bullet mol^{-1} \bullet s^{-2} = \sum_{i=0}^{2} f_i T^i \quad (20)$$

$$B_v = \sum_{i=0}^{2} g_i T^i \quad (21)$$

4. Conclusions

An approach is described for a rolling ball viscometer/densimeter universal calibration method that accounts for the effects of pressure, temperature, and fluid dependency for normal and branched alkanes ranging from octane to squalane. The equation for the calibration constant K presented here is valid over a wide range of viscosities from 0.4 to 1140 mPa•s observed with n-alkanes and branched alkanes, temperatures to 530 K, and pressures to 250 MPa. The effectiveness of this calibration equation is demonstrated through agreement between measured HXD and squalane viscosities and viscosities calculated using available reference correlations. Viscosities determined with a quadratic polynomial representation for K, which is typically used, deviate significantly from viscosities measured in the present study. The method used here obviates the

need to calibrate the viscometer with a fluid closely mimicking the viscosity profile of the fluid of interest. Current studies are in progress in our lab to test this calibration procedure/equation with other classes of pure fluids, such as aromatics and naphthenes, as well as complex, multicomponent mixtures, such as diesel or jet fuels.

Table 6. Parameters obtained for temperature-dependent FVT parameters, equations 20 and 21, used to calculate HXD, HMN, and squalane viscosities. Listed also are the Δ_{AAD} and Δ_{max} values associated with each fit of the data.

Fluid:	HXD	HMN	squalane
L/Å	0.6257	0.7234	0.6116
α/m^5•mol^{-1}•s^{-2}			
f_0	$1.8785 \cdot 10^{2}$	$9.7237 \cdot 10^{1}$	$1.4035 \cdot 10^{2}$
f_1	$-1.6509 \cdot 10^{-1}$	$1.9873 \cdot 10^{-1}$	1.0235
f_2	$1.0672 \cdot 10^{-5}$	$5.3395 \cdot 10^{-7}$	$-5.1969 \cdot 10^{-4}$
B_v			
g_0	$7.2932 \cdot 10^{-3}$	$2.5702 \cdot 10^{-2}$	$9.9603 \cdot 10^{-3}$
g_1	$-1.4469 \cdot 10^{-5}$	$-8.5122 \cdot 10^{-5}$	$-3.2631 \cdot 10^{-5}$
g_2	$1.2759 \cdot 10^{-8}$	$9.2029 \cdot 10^{-8}$	$3.2137 \cdot 10^{-8}$
Δ_{AAD}/%	1.4	3.5	5.9
Δ_{max}/%	3.7	7.5	16.4

Densities obtained in this study are reasonably predicted with the HTHP-GC-PC-SAFT EoS, however, deviations between experimental and calculated densities increase as the

component molecular weight increases or the extent of branching increases. Viscosities modeled using FVT in conjunction with HTHP-GC-PC-SAFT calculated densities are improved significantly by allowing two of the FVT parameters to vary with temperature. The improvement is especially significant for the branched alkanes that are expected to exhibit a strong, temperature-dependent free volume. Although temperature-dependent FVT parameters greatly improve viscosity predictions, the challenge remains to apply this methodology in a systematic manner to complex multicomponent mixtures.

Acknowledgments

This project has received funding from the European Union Horizon 2020 Research and Innovation program, Grant Agreement No 675528. The authors thank Joseph Roos (Afton), Joseph Remias (Afton), Joshua Moore (Afton), and Mark Devlin (Afton) for their helpful, technical discussions.

Supporting Information

Included in the SI are the data tables containing measured densities and viscosities obtained in this study, figures providing an overview of where original data were obtained, a brief overview of the RBVD volume calibration, equations and parameters for the density and viscosity correlations fit to our HMN data which are used for comparison to available literature data for this fluid, an example of how to use Group Contribution to calculate PC-SAFT parameters, and deviations plots comparing measured densities to those calculated with PC-SAFT.

References

1. Gupta, S.; Olson, J. D., Industrial Needs in Physical Properties. *Industrial & Engineering Chemistry Research* **2003,** 42, 6359-6374.

2. Hendriks, E.; Kontogeorgis, G. M.; Dohrn, R.; de Hemptinne, J.-C.; Economou, I. G.; Žilnik, L. F.; Vesovic, V., Industrial Requirements for Thermodynamics and Transport Properties. *Industrial & Engineering Chemistry Research* **2010,** 49, 11131-11141.

3. Caudwell, D. R.; Trussler, J. P. M.; Vesovic, V.; Wakeham, W. A., Viscosity and density of five hydrocarbon liquids at pressures up to 200 MPa and temperatures up to 473 K. *Journal of Chemical and Engineering Data* **2009,** 54, 359-366.

4. Ciotta, F.; Maitland, G.; Smietana, M.; Trussler, J. P. M.; Vesovic, V., Viscosity and density of carbon dioxide + 2,6,10,15,19,23-hexamethyltetracosane (squalane). *Journal of Chemical and Engineering Data* **2009,** 54, 2436-2443.

5. Aquing, M.; Ciotta, F.; Creton, B.; Féjean, C.; Pina, A.; Dartiguelongue, C.; Trussler, J. P. M.; Vignais, R.; Lugo, R.; Ungerer, P.; Nieto-Draghi, C., Composition analysis and viscosity prediction of complex fuel mixtures using a molecular-based approach. *Energy & Fuels* **2012,** 26, 2220-2230.

6. Schmidt, K. A. G.; Pagnutti, D.; Curran, M. D.; Singh, A.; Trussler, J. P. M.; Maitland, G.; McBride-Wright, M., New experimental data and reference models for the viscosity and density of squalane. *Journal of Chemical and Engineering Data* **2015,** 60, 137-150.

7. Comuñas, M. J. P.; Paredes, X.; Gaciño, F. M.; Fernández, J.; Bazile, J. P.; Boned, C.; Daridon, J. L.; Galliero, G.; Pauly, J.; Harris, K. R., Viscosity measurements for squalane at high pressures to 350 MPa from T = (293.15 to 363.15) K. *Journal of Chemical Thermodynamics* **2014,** 69, 201-208.

8. Harris, K. R., Temperature and pressure dependence of the viscosities of 2-ethylhexyl benzoate, bis(2-ethylhexyl) phthalate, 2,6,10,15,19,23-hexamethyltetracosane (squalane), and diisodecyl phthalate. *Journal of Chemical and Engineering Data* **2009,** 54, 2729-2738.

9. Baled, H. O. Density and viscosity of hydrocarbons at extreme conditions associated with ultra-deep reservoirs-measurements and modeling. PhD Thesis, University of Pittsburgh, 2012.

10. Baled, H. O.; Xing, D.; Katz, H.; Tapriyal, D.; Gamwo, I. K.; Soong, Y.; Bamgbade, B. A.; Wu, Y.; Liu, K.; McHugh, M. A.; Enick, R. M., Viscosity of n-hexadecane, n-octadecane and n-eicosane at pressures up to 243 MPa and temperatures up to 534 K. *Journal of Chemical Thermodynamics* **2014,** 72, 108-116.

11. Paredes, X.; Fandiño, O.; Comuñas, M. J. P.; Pensado, A. S.; Fernández, J., Study of the effects of pressure on the viscosity and density of diisodecyl phthalate. *Journal of Chemical Thermodynamics* **2009,** 41, 1007-1015.

12. Pensado, A. S.; Commuñas, M. J. P.; Lugo, L.; Fernández, J., High-pressure characterization of dynamic viscosity and derived properties for squalane and two pentaerythritol ester lubricants: Pentaerythritol tetra-2-ethylhexanoate and pentaerythritol tetranonanoate. *Industrial and Engineering Chemistry Research* **2006,** 45, 2394-2404.

13. Rowane, A. J.; Mallepally, R. M.; Bamgbade, B. A.; Newkirk, M. S.; Baled, H. O.; Burgess, W. A.; Gamwo, I. K.; Tapriyal, D.; Enick, R. M.; McHugh, M. A., High-temperature, high-pressure viscosities and densities of toluene. *Journal of Chemical Thermodynamics* **2017,** 115, 34-46.

14. Sato, Y.; Yoshioka, H.; Aikawa, S.; Smith, R. L., A digital variable-angle rolling-ball viscometer for measurement of viscosity, density, and bubble-point pressure of CO_2 and organic liquid mixtures. *International Journal of Thermophysics* **2010,** 31, 1896-1903.

15. Baled, H. O.; Tapriyal, D.; Morreale, B. D.; Soong, Y.; Gamwo, I. K.; Krukonis, V.; Bamgbade, B. A.; Wu, Y.; McHugh, M. A.; Burgess, W. A.; Enick, R. M., Exploratory characterization of a perfluoropolyether oil as a possible viscosity standard at deepwater production conditions of 533 K and 241 MPa. *International Journal of Thermophysics* **2013,** 34, 1845-1864.

16. Tomida, D.; Kumagai, A.; Yokoyama, C., Viscosity Measurements and Correlation of the Squalane + CO_2 Mixtures. *International Journal of Thermophysics* **2007,** 28, 133-145.

17. Assael, M. J.; Kalyva, A. E.; Monogenidou, S. A.; Huber, M. L.; Perkins, R. A.; Friend, D. G.; May, E. F., Reference values and reference correlations for the thermal conductivity and viscosity of fluids. *Journal of Physical and Chemical Reference Data* **2018,** 47, 021501.

18. Meng, X. Y.; Sun, Y. K.; Cao, F. L.; Wu, J. T.; Vesovic, V., Reference correlation of the viscosity of n-hexadecane from the triple point to 673 K and up to 425 MPa. *Journal of Physical and Chemical Reference Data* **2018,** 47, 033102.

19. Mylona, S. K.; Assael, M. J.; Commuñas, M. J. P.; Paredes, X.; Gaciño, F. M.; Fernández, J.; Bazile, J. P.; Boned, C.; Daridon, J. L.; Galliero, G.; Pauly, J.; Harris, K. R., Reference correlations for the density and viscosity of squalane from 273 to 473 K at pressures to 200 MPa. *Journal of Physical and Chemical Reference Data* **2014,** 43, 013104.

20. Bair, S., The high pressure rheology of some simple model hydrocarbons. *Proceedings of the Institution of Mechanical Engineers, Part J, Journal of engineering tribology* **2002,** 216, 139-149.

21. Bair, S., Reference liquids for quantitative elastohydrodynamics: selection and rheological characterization. *Tribology Letters* **2006,** 22, 197-206.

22. Bair, S.; McCabe, C.; Cummings, P., T., Calculation of viscous EHL traction for squalane using molecular simulation and rheometry. *Tribology Letters* **2002,** 13, 251-254.

23. Bamgbade, B. A.; Wu, Y.; Burgess, W. A.; Tapriyal, D.; Gamwo, I. K.; Baled, H. O.; Enick, R. M.; McHugh, M. A., High-temperature, high-pressure volumetric properties of propane, squalane, and their mixtures: Measurement and PC-SAFT modeling. *Industrial and Engineering Chemistry Research* **2015,** 54, 6804-6811.

24. Fandiño, O.; Lugo, L.; Comuñas, M. J. P.; López, E. R.; Fernández, J., Temperature and pressure dependences of volumetric properties of two poly(propylene glycol) dimethyl ether lubricants. *Journal of Chemical Thermodynamics* **2010,** 42, 84-89.

25. Fandiño, O.; Pensado, A. S.; Lugo, L.; Commuñas, M. J. P.; Fernández, J., Compressed liquid densities of squalane and pentaerythritol tetra(2-ethylhexanoate). *Journal of Chemical and Engineering Data* **2005,** 50, 939-946.

26. Hata, H.; Tamoto, Y., High-pressure viscosity measurments for various lubricants, and prediction of atmospheric pressure-viscosity coefficient from the easily measurable properties of lubricant (Part 2) - Results of various synthetic lubricating oils. *Journal of Japanese Society of Tribologists* **2010,** 55, 647-658.

27. Krahn, U. G.; Luft, G., Viscosity of several liquid hydrocarbons in the temperature range 298-453 K at pressures up to 200 MPa. *Journal of Chemical and Engineering Data* **1994,** 39, 670-672.

28. Kumagai, A.; Takahashi, S., Viscosity and density of liquid mixtures of n-alkanes with squalane. *International Journal of Thermophysics* **1995,** 16, 773-779.

29. Kuss, E. V.; Golly, H., Das Viskositäts-Druckverhalten von Gas-Flüssigkeitslösungen. *Berichte der Bunsen - Gesellschaft fur Physikalische Chemie* **1972,** 76, 131-138.

30. Mylona, S., K.; Assael, M., J.; Antoniadis, K., D.; Polymatidou, S., K.; Karagiannidis, L., Measurements of the viscosity of bis(2-ethylhexyl) sebacate, squalane, and bis(2-ethylhexyl) phthalate between (283 and 363) K at 0.1 MPa. *Journal of Chemical and Engineering Data* **2013,** 58, 2805-2808.

31. Canet, X.; Daugé, P.; Baylaucq, A.; Boned, C.; Zéberg-Mikkelsen, C. K.; Quiñones-Cisneros, S. E.; Stenby, E. H., Density and viscosity of the 1-methylnaphthalene + 2,2,4,4,6,8,8-heptamethylnonane system from 293.15 to 353.15 K at pressures up to 100 MPa. *International Journal of Thermophysics* **2001,** 22, 1669-1689.

32. Et-Tahir, A.; Boned, C.; Lagourette, B.; Xans, P., Determination of the viscosity of various hydrocarbons and mixtures of hydrocarbons versus temperature and pressure. *International Journal of Thermophysics* **1995,** 16, 1309-1334.

33. Fermeglia, M.; Torriano, G., Density, viscosity, and refractive index for binary systems of n-C16 and four nonlinear alkanes at 298.15 K. *Journal of Chemical and Engineering Data* **1999,** 44, 965-969.

34. Knothe, G.; Steidley, K. R., Kinematic viscosity of biodiesel fuel and related compounds. Influence of compound structure and comparison to petrodiesel fuel components. *Fuel* **2005,** 84, 1059-1065.

35. Luning Prak, D. J.; Jones, M. H.; Cowart, J. S.; Trulove, P. C., Density, viscosity, speed of sound, bulk modulus, surface tension, and flash point of binary mixtures of 2,2,4,6,6-pentamethylheptane and 2,2,4,4,6,8,8 heptamethylnonane at (293.15 to 373.15) K and 0.1 MPa and comparisons with alcohol-to-jet fuel. *Journal of Chemical and Engineering Data* **2015,** 60, 1157-1165.

36. Lunning Prak, D. J.; Alexandre, S. M.; Cowart, J. S.; Trulove, P. C., Density, viscosity, speed of sound, bulk modulus, surface tension, and flash point of binary mixtures of n‑dodecane with 2,2,4,6,6-pentamethylheptane or 2,2,4,4,6,8,8-heptamethylnonane. *Journal of Chemical and Engineering Data* **2014,** 59, 1334-1346.

37. Zéberg-Mikkelsen, C. K.; Barrouhou, M.; Baylaucq, A.; Boned, C., Measurements of the viscosity and density versus temperature and pressure for the binary system methylcyclohexane + 2,2,4,4,6,8,8-heptamethylnonane. *High Temperatures High Pressures* **2002,** 34, 591-601.

38. Liu, K.; Wu, Y.; McHugh, M. A.; Baled, H.; Enick, R. M.; Morreale, B. D., Equation of state modeling of high-pressure, high-temperature hydrocarbon density data. *The Journal of Supercritical Fluids* **2010,** 55, 701-711.

39. Wu, Y.; Bamgbade, B.; Liu, K.; McHugh, M. A.; Baled, H.; Enick, R. M.; Burgess, W. A.; Tapriyal, D.; Morreale, B. D., Experimental measurements and equation of state modeling of liquid densities for long-chain n-alkanes at pressures to 265 MPa and temperatures to 523 K. *Fluid Phase Equilibria* **2011,** 311, 17-24.

40. Seiji Sawamura, T. Y. In *Rolling-Ball viscometer for studying water and aqueous solutions under high pressure* 14th International Conference on the Properties of Water and Steam, Kyoto, 2004; Kyoto, 2004; pp 429-434.

41. Kermis, T. W.; Li, D.; Guney-Altay, O.; Park, I.-H.; van Zanten, J. H.; McHugh, M. A., High-pressure dynamic light scattering of poly(ethylene-co-1-butene) in ethane, propane, butane, and pentane at 130 °C and kilobar pressures. *Macromolecules* **2004,** 37, 9123-9131.

42. Hubbard, R. M.; Brown, G. G., The rolling ball viscometer. *Industrial and Engineering Chemistry* **1943,** 15, 212-218.

43. Lewis, H. W., Calibration of the rolling ball viscometer. *Analytical Chemistry* **1953,** 25, 507-508.

44. Izuchi, M.; Nishibata, K., A high pressure rolling-ball viscometer up to 1 GPa. *Japanese Journal of Applied Physics* **1986,** 25, 1091-1096.

45. Bair, S.; Yamaguchi, T., The equation of state and the temperature, pressure, an shear dependence of viscosity for a highly viscous reference liquid, dipentaerythritol hexaisononanoate. *Journal of Tribology* **2017,** 139, 011801.

46. Special Metals: Inconel 718. http://www.specialmetals.com/assets/smc/documents/inconel_alloy_718.pdf (11/12/2018),

47. Wu, J.; Shan, Z.; Asfour, A.-F. A., Viscometric properties of multicomponent liquid n-alkane systems. *Fluid Phase Equilibria* **1998,** 143, 263-274.

48. Knapstead, B.; Skjøsvlk, P. A.; Øye, H. A., Viscosity of pure hydrocarbons. *Journal of Chemical and Engineering Data* **1989,** 34, 37-43.

49. Romeo, R.; Lemmon, E. W., Helmholtz equation of state for hexadecane. **Unpublished**.

50. Dymond, J. H.; Young, K. J.; Isdale, J. D., Transport properties of nonelectrolyte liquid mixtures--II. Viscosity coefficients for the n-hexane + n-hexadecane system at temperatures from 25 to 100ºC at pressures up to the freezing pressure or 500 MPa. *International Journal of Thermophysics* **1980,** 1, 345-373.

51. Tanaka, Y.; Hosokawa, H.; Kubota, H.; Makita, T., Viscosity and density of binary mixtures of cyclohexane with *n*-octane, *n*-dodecane, and *n*-hexadecane under high pressures. *International Journal of Thermophysics* **1991,** 12, 245-264.

52. Kleinschmidt, R. V.; Bradbury, D.; Mark, M. *Viscosity and density of over 40 lubricating fluids of known composition at pressures to 150,000 psi and temperatures to 425 F*; The American Society of Mechanical Engineers: New York, 1953.

53. Chang, J.-S.; Lee, M.-J.; Lin, H., Densities of binary mixtures of hexadecane with m-xylene and tetralin from 333 K to 413 K and pressures up to 30 MPa. *Journal of Chemical and Engineering Data* **1998,** 43, 233-237.

54. Outcault, S.; Laesecke, A.; Fortin, T. J., Density and speed of sound measurements of hexadecane. *Journal of Chemical Thermodynamics* **2010,** 42, 700-706.

55. Banipal, T. S.; Garg, S. K.; Ahluwalia, J. C., Heat capacities and densities of liquid n-octane, n-nonane, n-decane, and n-hexadecane at temperatures from 318.15 K to 373.15 K and at pressures up to 10 MPa. *Journal of Chemical Thermodynamics* **1991,** 23, 923-931.

56. Dymond, J. H.; Young, K. J., p, ρ, T behaviour for n-hexane + n-hexadecane in the range 298 to 373 K and 0.1 to 500 MPa. *Journal of Chemical Thermodynamics* **1979,** 11, 887-895.

57. Glaser, M.; Peters, C. J.; Van der Kool, H. J.; Lichtenthaler, R. N., Phase equilibira of (methane + *n*-hexadecane) and (p, V_m, T) of *n*-hexadecane. *Journal of Chemical Thermodynamics* **1985,** 17, 803-815.

58. Würflinger, A.; Mondieig, D.; Rajabalee, F.; Cuevas-Diarte, M. A., *pVT* measurements and related studies on the binary system nC$_{16}$H$_{34}$ - nC$_{17}$H$_{36}$ and on nC$_{18}$H$_{38}$ at high pressures. *Zeitschrift fur Naturforschung* **2001,** 56, 626-634.

59. Amorim, J. A.; Chiavone-Filho, O.; Paredes, M. L. L.; Rajagopal, K., High-pressure density measurements for the binary system cyclohexane + n-hexadecane in the temperature range of (318.15 to 413.15) K. *Journal of Chemical and Engineering Data* **2007,** 52, 613-618.

60. Gouel, P., Masse volumique des alcanes (C$_6$ à C$_{16}$) des cycliques et alkyl-benzenes. *Bulletin des centres de recherches exploration-production Elf-Aquitaine* **1978,** 2, 211-225.

61. Matthews, M. A.; Rodden, J. B.; Akgerman, A., High-temperature diffusion, viscosity, and density measurements in n-hexadecane. *Journal of Chemical and Engineering Data* **1987,** 32, 317-319.

62. Kuss, E.; Taslimi, M., *p*,*V*,*T*-Messungen an zwanzig organischen Flussigkeiten. *Chemie Ingenieur Technik* **1970,** 17, 1073-1120.

63. Barrouhou, M.; Zéberg-Mikkelsen, C. K.; Baylaucq, A.; Boned, C., High-pressure viscosity and density measurements for the asymmetric binary system cis-decalin + 2,2,4,4,6,8,8-heptamethylnonane. *International Journal of Thermophysics* **2003,** 24, 937-952.

64. Lunning Prak, D. J.; Morris, R. E.; Cowart, J. S.; Hamilton, L. J.; Trulove, P. C., Density, viscosity, speed of sound, bulk modulus, surface tension, and flash point of direct sugar to

hydrocarbon diesel (DSH-76) and binary mixtures of n‑hexadecane and 2,2,4,6,6-pentamethylheptane. *Journal of Chemical and Engineering Data* **2013,** 58, 3536-3544.

65. Lunning Prak, D. J.; Graft, S. L.; Johnson, T. R.; Cowart, J. S., Density, viscosity, speed of sound, bulk modulus, surface tension,and flash point of binary mixtures of n-hexylbenzene (1) or n-butylbenzene (1) in 2,2,4,6,6-pentamethylheptane (2) or ,2,4,4,6,8,8-heptamethylnonane (2) at 0.1 MPa. *Journal of Chemical and Engineering Data* **2018,** 63, 3503-3519.

66. Huber, M. L. *Preliminary models for viscosity, thermal conductivity, and surface tension of pure fluid constituents of selected diesel surrogate fuels*; National Institute of Standards: 2017.

67. Rajagopal, K.; Andrade, L. L. P. R.; Paredes, M. L. L., High-pressure viscosity measurements for the binary system cyclohexane + n-hexadecane in the temperature range of (318.15 to 413.15) K. *Journal of Chemical and Engineering Data* **2009,** 54, 2967-2970.

68. Ducoulombier, D.; Zhou, H.; Boned, C.; Peyrelasse, J.; Saint-Guirons, H.; Xans, P., Pressure (1-1000 bars) and temperature (20-100°C) dependence of the viscosity of liquid hydrocarbons. *The Journal of Physical Chemistry* **1986,** 90, 1692-1700.

69. Rastorguev, Y. L.; Keramidi, A. S., Viskosität von Alkanen. *Izvestiia Vysshikh Uchebnykh Zavedenii. Neft Gaz* **1972,** 1, 61-66.

70. Mohammed, M.; Ciotta, F.; Trussler, J. P. M., Viscosities and densities of binary mixtures of hexadecane with dissolved methane or carbon dioxide at temperatures from (298 to 473) K and at pressures up to 120 MPa. *Journal of Chemical and Engineering Data* **2017,** 62, 422-239.

71. Communãs, M. J. P.; Paredes, X.; Gaciño, F. M.; Fernández, J.; Bazile, J. P.; Boned, C.; Daridon, J. L.; Galliero, G.; Pauly, J.; Harris, K. R.; Assael, M. J.; Mylona, S. K., Reference correlation of the viscosity of squalane from 273 to 373 K at 0.1 MPa. *Journal of Physical and Chemical Reference Data* **2013,** 42, 033101.

72. Burgess, W. A.; Tapriyal, D.; Gamwo, I. K.; Wu, Y.; McHugh, M. A.; Enick, R. M., New group-contribution parameters for the calculation of PC-SAFT parameters for use at pressures to 276 MPa and temperatures to 533 K. *Industrial and Engineering Chemistry Research* **2014,** 53, 2520-2528.

73. Burgess, W. A.; Tapriyal, D.; Gamwo, I. K.; Morreale, B. D.; McHugh, M. A.; Enick, R. M., Viscosity models based on the free volume and frictional theories for systems at pressures to 276 MPa and temperatures to 533 K. *Industrial and Engineering Chemistry Research* **2012,** 51, 16721-16733.

74. Allal, A.; Boned, C.; Baylaucq, A., Free-volume viscosity model for fluids in the dense and gaseous states. *Physical Review E* **2001,** 64, 011203.

75. Polishuk, I.; Yitzhak, A., Modeling viscosities of pure compounds and their binary mixtures using modified Yarranton-Satyro correlation and free volume theory coupled with SAFT + cubic EoS. *Industrial and Engineering Chemistry Research* **2014,** 53, 959-971.

76. Yashi, U., Interrelationships between *P-V-T* and flow behavior of linear and nonlinear hydrocarbons. *Polymer Engineering and Science* **1998,** 38, 464-470.